

CAUSAL COVARIATE SHIFT CORRECTION USING FISHER INFORMATION PENALTY

Behraj Khan^{1,2}, Behroz Mirza³, and Tahir Syed¹

¹Institute of Business Administration Karachi, Pakistan
 {behrajkhana, tqsyed}@iba.edu.pk

²National University of Computer and Emerging Sciences, Pakistan

³Habib University, Karachi, Pakistan {behroz.mirza}@sse.habib.edu.pk

ABSTRACT

Evolving feature densities across batches of training data bias cross-validation, making model selection and assessment unreliable (Sugiyama & Kawanabe (2012)). This work takes a distributed density estimation angle to the training setting where data are temporally distributed. *Causal Covariate Shift Correction (C³)*, accumulates knowledge about the data density of a training batch using Fisher Information, and using it to penalize the loss in all subsequent batches. The penalty improves accuracy by 12.9% over the full-dataset baseline, by 20.3% accuracy at maximum in batchwise and 5.9% at minimum in foldwise benchmarks.

1 BACKGROUND

In learning systems over big data, the training dataset may not be completely available at the same time and place. Therefore, such a real-world setting fails the assumption of the classical machine learning model of independent and identically distributed (iid) source and target data. Such problems are characterized as distribution shift Quiñero-Candela et al. (2008), most commonly as *covariate shift* Cortes et al. (2008); Sugiyama et al. (2007b); Moreno-Torres et al. (2012); Vigneron et al. (2010), where training and test feature distributions differ. In continual or streaming applications, we may encounter what we term *causal covariate shift*, causality being defined as the immutability of the batching sequence van den Oord et al. (2016).

2 METHOD DEVELOPMENT

Measuring the amount of shift between distribution of different batches requires the use of a metric on the space of probability distributions. The natural choice is the relative entropy / Kullback-Leibler divergence Kullback & Leibler (1951) as a quasi-metric because of its theoretical proximity with the cross entropy network loss, and because the ordering among batches imposes a natural direction on the computation. The usual mean-field formulation of the KL-divergence uses a Gaussian $q(\theta)$ distribution, parametrised with the covariance matrix of the network parameters. This term involves the Hessian of the derivatives of the parameters, and the high-dimensionality of the latter renders its computation intractable. Recent inference literature Pascanu & Bengio (2013) suggests an approximation by the Fisher Information Matrix (FIM), a quantity that can be derived using the variance and expected value of the function of interest Nishiyama (2019).

Let us consider a model with parameters θ and a likelihood function $p(X | \theta)$, where X is observed data. The estimate of true parameter θ can be found by using estimator $\hat{\theta}$. The Fisher information $I(\theta)$ can be defined as the expected value of the negative hessian of the log-likelihood function $I(\theta) = \mathbb{E} \left[-\frac{\partial^2 \log p(X|\theta)}{\partial \theta \partial \theta^T} \right]$. The Cramér-Rao Lower Bound (CRLB) states that for any unbiased estimator $\hat{\theta}$, the covariance matrix $V(\hat{\theta})$ satisfies the matrix inequality property: $V(\hat{\theta}) \succeq I^{-1}(\theta)$.

Now let us assume $q(\hat{\theta})$ as Gaussian distribution function to be estimated around parameter θ mean and variance-covariance matrix $V(\hat{\theta})$ in such manner that: $q(\hat{\theta}) \approx \mathcal{N}(\theta, V(\hat{\theta}))$. The D_{KL} for

source to target distribution is defined by $D_{KL}(P \parallel Q) = \sum_y P(y|x) \log \left(\frac{P(y|x)}{Q(y|x)} \right)$, with $P(y|x)$ as the classifier output, and $Q(y|x)$ as Normal with means μ_P and μ_Q and variances σ_P^2 and σ_Q^2 .

The D_{KL} can be approximated as:

$$D_{KL}(p(\theta) \parallel q(\hat{\theta})) \approx \int p(\theta) \log \left(\frac{p(\theta)}{\mathcal{N}(\theta, V(\hat{\theta}))} \right) d\theta \quad (1)$$

Our method approximates the $V(\hat{\theta})$ by $I(\theta)$, with detail in appendix A:

$$I(\theta) = -\mathbb{E} \left[\frac{\partial^2 \log P(X; \theta)}{\partial \theta^2} \right] \quad (2)$$

An important result Courtade (2016) shows that Fisher information remains strictly upper bounded by entropy, such as the increasing frontiers in Vigneron et al. (2010). We propose a massive decrease in computation by using the FIM instead of the entire divergence term. The formulation follows the familiar Tikhonov mechanism of weighted penalty addition.

$$\mathcal{L}(x, y; \theta) = - \int P(y(x)) \log(P(y|x; \theta)) d\theta - \lambda \times \int \frac{\partial^2 \log p(X | \theta)}{\partial \theta \partial \theta^T} d\theta \quad (3)$$

The penalty bears familiar derivative operations as gradient descent, and therefore does not alter the algorithm’s complexity class. The strength of the penalty, λ , is akin to a continuously-variable Forget gate of an LSTM. Setting it to zero means that gradients for a batch are computed independent of any previous batch, while the deviation between the distribution of the two gradients is increasingly penalized with a larger λ . We present the calibration of λ in Fig. 1 of the appendix.

3 EXPERIMENTS

To compare the effectiveness of C^3 we used 40 real-world benchmarking datasets. We use 13 image-based datasets benchmarks and 27 binary datasets from KEEL repository Alcalá-Fdez et al. (2011) to evaluate our method.

Dataset	Baseline	SOTA				Ours	$\Delta_1 = C^3 - CV$ $\Delta_2 = C^3 - DIW$	
	CV	IW	IWCV	KMM	DIW	C^3	Δ_1 (%)	Δ_2 (%)
MNIST	94.8	85.1	76.9	11.8	98.0	97.9	↑ 3.1	↓ 0.1
Permuted-MNIST	95.1	67.8	75.4	11.2	84.7	97.6	↑ 2.5	↑ 12.9
Fashion-MNIST	82.3	80.2	72.3	10.3	87.2	88.4	↑ 6.1	↑ 1.2
Kuzushiji-MNIST	77.1	78.3	74.2	10.2	86.7	89.2	↑ 12.1	↑ 2.5
CIFAR-10	71.5	79.8	69.9	9.61	80.4	87.7	↑ 16.2	↑ 7.3
CIFAR-100	38.2	44.6	51.7	8.53	53.6	58.7	↑ 14.1	↑ 5.1
CIFAR10-C	63.9	69.1	60.1	7.87	69.4	73.3	↑ 9.40	↑ 3.9
CIFAR100-C	28.8	18.7	16.9	5.37	32.6	39.4	↑ 10.6	↑ 7.2

Table 1: C^3 vs SOTA.

4 CONCLUSIONS

1. Correcting causal covariate shift through C^3 also helps in natural covariate shift correction. C^3 ’s accuracy improves for a complete in-memory dataset with natural covariate shift such as Kuzushiji-MNIST, CIFAR10-C, CIFAR100-C, and Permuted-MNIST.
2. We report increases of 16.2%, 14.2%, 12.1%, 6.1%, 2.5% and 3.1% accuracy as compares to standard CV (cross-validation) in a batchwise setup.
3. We outperform SOTA benchmarks with improvements of 12.9%, 7.3%, and 5.1% accuracy when we have access to the complete dataset.
4. C^3 also outperforms by 9.4%, 7.7%, and 7.4% accuracy improvement in k-fold setting CV.

Empirical results across several experimental baselines present evidence of our method serving as a short tether between varying covariate distributions, whenever data are distributed across batches, or experimentally as folds. The work therefore may be of immediate utility for federated or continual learning, or in AutoML.

URM STATEMENT

We acknowledge that all authors of this work meet the URM criteria of ICLR 2024 Tiny Papers Track.

REFERENCES

- Jesús Alcalá-Fdez, Alberto Fernández, Julián Luengo, Joaquín Derrac, Salvador García, Luciano Sánchez, and Francisco Herrera. Keel data-mining software tool: data set repository, integration of algorithms and experimental analysis framework. *Journal of Multiple-Valued Logic & Soft Computing*, 17, 2011.
- Tarin Clanuwat, Mikel Bober-Irizar, Asanobu Kitamoto, Alex Lamb, Kazuaki Yamamoto, and David Ha. Deep learning for classical japanese literature. *arXiv preprint arXiv:1812.01718*, 2018.
- Adam Coates, Andrew Ng, and Honglak Lee. An analysis of single-layer networks in unsupervised feature learning. In *Proceedings of the fourteenth international conference on artificial intelligence and statistics*, pp. 215–223. JMLR Workshop and Conference Proceedings, 2011.
- Corinna Cortes, Mehryar Mohri, Michael Riley, and Afshin Rostamizadeh. Sample selection bias correction theory. In *Algorithmic Learning Theory: 19th International Conference, ALT 2008, Budapest, Hungary, October 13-16, 2008. Proceedings 19*, pp. 38–53. Springer, 2008.
- Thomas A Courtade. Monotonicity of entropy and fisher information: a quick proof via maximal correlation. *arXiv preprint arXiv:1610.04174*, 2016.
- Tongtong Fang, Nan Lu, Gang Niu, and Masashi Sugiyama. Rethinking importance weighting for deep learning under distribution shift. *Advances in neural information processing systems*, 33: 11996–12007, 2020.
- Li Fei-Fei, Rob Fergus, and Pietro Perona. Learning generative visual models from few training examples: An incremental bayesian approach tested on 101 object categories. *Computer Vision and Pattern Recognition Workshop*, 2004.
- Ian J Goodfellow, Mehdi Mirza, Da Xiao, Aaron Courville, and Yoshua Bengio. An empirical investigation of catastrophic forgetting in gradient-based neural networks. *arXiv preprint arXiv:1312.6211*, 2013.
- Arthur Gretton, Alex Smola, Jiayuan Huang, Marcel Schmittfull, Karsten Borgwardt, Bernhard Schölkopf, et al. Covariate shift by kernel mean matching. *Dataset shift in machine learning*, 3(4):5, 2009.
- Dan Hendrycks and Thomas Dietterich. Benchmarking neural network robustness to common corruptions and perturbations. *Proceedings of the International Conference on Learning Representations*, 2019.
- Jiayuan Huang, Arthur Gretton, Karsten Borgwardt, Bernhard Schölkopf, and Alex Smola. Correcting sample selection bias by unlabeled data. *Advances in neural information processing systems*, 19, 2006.
- Alex Krizhevsky, Geoffrey Hinton, et al. Learning multiple layers of features from tiny images. 2009.
- Solomon Kullback and Richard A Leibler. On information and sufficiency. *The annals of mathematical statistics*, 22(1):79–86, 1951.
- Yann LeCun. The mnist database of handwritten digits. <http://yann.lecun.com/exdb/mnist/>, 1998.
- Jose García Moreno-Torres, José A Sáez, and Francisco Herrera. Study on the impact of partition-induced dataset shift on k -fold cross-validation. *IEEE Transactions on Neural Networks and Learning Systems*, 23(8):1304–1312, 2012.
- Norman Mu and Justin Gilmer. Mnist-c: A robustness benchmark for computer vision. *arXiv preprint arXiv:1906.02337*, 2019.

- Yuval Netzer, Tao Wang, Adam Coates, Alessandro Bissacco, Bo Wu, and Andrew Y Ng. Reading digits in natural images with unsupervised feature learning. 2011.
- Tomohiro Nishiyama. A new lower bound for kullback-leibler divergence based on hammersley-chapman-robbins bound. *arXiv preprint arXiv:1907.00288*, 2019.
- Razvan Pascanu and Yoshua Bengio. Revisiting natural gradient for deep networks. *arXiv preprint arXiv:1301.3584*, 2013.
- Joaquin Quiñero-Candela, Masashi Sugiyama, Anton Schwaighofer, and Neil D Lawrence. *Dataset shift in machine learning*. Mit Press, 2008.
- Masashi Sugiyama and Motoaki Kawanabe. *Machine learning in non-stationary environments: Introduction to covariate shift adaptation*. MIT press, 2012.
- Masashi Sugiyama, Matthias Krauledat, and Klaus-Robert Müller. Covariate shift adaptation by importance weighted cross validation. *Journal of Machine Learning Research*, 8(5), 2007a.
- Masashi Sugiyama, Shinichi Nakajima, Hisashi Kashima, Paul Buenau, and Motoaki Kawanabe. Direct importance estimation with model selection and its application to covariate shift adaptation. *Advances in neural information processing systems*, 20, 2007b.
- Aäron van den Oord, Sander Dieleman, Heiga Zen, Karen Simonyan, Oriol Vinyals, Alex Graves, Nal Kalchbrenner, Andrew W. Senior, and Koray Kavukcuoglu. Wavenet: A generative model for raw audio. *CoRR*, abs/1609.03499, 2016. URL <http://arxiv.org/abs/1609.03499>.
- Vincent Vigneron, Tahir Q Syed, Georgia Barlovatz-Meimon, Michel Malo, Christophe Montagne, and Sylvie Lelandais. Adaptive filtering and hypothesis testing: Application to cancerous cells detection. *Pattern recognition letters*, 31(14):2214–2224, 2010.
- Han Xiao, Kashif Rasul, and Roland Vollgraf. Fashion-mnist: a novel image dataset for benchmarking machine learning algorithms. *arXiv preprint arXiv:1708.07747*, 2017.

A APPENDIX

In this section, we describe the relationship between relative entropy and fisher information. We also present the baselines, datasets details, C^3 batchwise performance λ selection details, and experimental setup.

A.1 REPRESENTING THE CURRENT DERIVATIVE WITH THE FISHER INFORMATION MATRIX

Let us consider having a model with parameter θ and a likelihood function $p(X | \theta)$, where X is observed data. The estimate of true parameter θ can be found by using estimator $\hat{\theta}$. The Fisher information $I(\theta)$ can be defined as the expected value of the negative hessian of the log-likelihood function.

$$I(\theta) = \mathbb{E} \left[-\frac{\partial^2 \log p(X | \theta)}{\partial \theta \partial \theta^T} \right] \quad (4)$$

The Cramér-Rao Lower Bound (CRLB) states that for any unbiased estimator $\hat{\theta}$, the variance-covariance matrix $V(\hat{\theta})$ satisfies the inequality property:

$$V(\hat{\theta}) \succeq I^{-1}(\theta) \quad (5)$$

The symbol \succeq represents the following matrix inequality $V(\hat{\theta}) - I^{-1}(\theta)$ positive and semi-definite.

Now let us assume $q(\hat{\theta})$ as Gaussian distribution function to be estimated around parameter θ mean and variance-covariance matrix $V(\hat{\theta})$ in such manner that:

$$q(\hat{\theta}) \approx \mathcal{N}(\theta, V(\hat{\theta})) \quad (6)$$

We have a model $f(x)$ which outputs a target distribution $Q(y|x)$ for each given input x . The D_{KL} divergence for source to target distribution can be found by $D_{KL}(P || Q) = \sum_y P(y|x) \log \left(\frac{P(y|x)}{Q(y|x)} \right)$.

Considering y as continuous target variable, $P(y|x)$ and $Q(y|x)$ as Gaussian distributions with means μ_P and μ_Q and variances σ_P^2 and σ_Q^2 .

Relative entropy can be computed in closed form using mean-variance of source and target distribution as follows:

$$D_{KL}(P || Q) = \frac{1}{2} \left[\log \left(\frac{\sigma_Q^2}{\sigma_P^2} \right) + \frac{\sigma_P^2 + (\mu_P - \mu_Q)^2}{\sigma_Q^2} - 1 \right] \quad (7)$$

The D_{KL} can be approximated as:

$$D_{KL}(p(\theta) || q(\hat{\theta})) \approx \int p(\theta) \log \left(\frac{p(\theta)}{\mathcal{N}(\theta, V(\hat{\theta}))} \right) d\theta \quad (8)$$

With the help of CRLB we can replace $V(\hat{\theta})$ with $I^{-1}(\theta)$ as $V(\hat{\theta}) \succeq I^{-1}(\theta)$, we get:

$$D_{KL}(p(\theta) || q(\hat{\theta})) \approx \int p(\theta) \log \left(\frac{p(\theta)}{\mathcal{N}(\theta, I^{-1}(\theta))} \right) d\theta \quad (9)$$

which is the estimation of relative entropy by using a variance-covariance matrix of estimated parameters with the help of FIM.

A.2 THE FISHER INFORMATION MATRIX AS AN APPROXIMATION OF VARIATIONAL POSTERiors

Before introducing the penalty term which is one of our contributions we investigated the relation between relative entropy (D_{KL}) and FIM. Lets assume that θ is estimated parameter for given input data folds i.e $(X_1, X_2, X_3, \dots, X_n)$ with a probability function $P(x; \theta)$. By using an unbiased estimator $\hat{\theta}(X_1, X_2, \dots, X_n)$ of θ , the variance estimator satisfies the following CRLB property.

$$\sigma^2(\hat{\theta}) \geq \frac{1}{nI(\theta)} \quad (10)$$

where $I(\theta)$ is Fisher information and n is sample size which can be described as:

$$I(\theta) = -\mathbb{E} \left[\frac{\partial^2 \log P(X; \theta)}{\partial \theta^2} \right] \quad (11)$$

It is crucial to understand the relation of FIM to D_{KL} (D_{KL}). We can find D_{KL} between source to target distributions $P(x)$ and $Q(x)$ with the same support set of X with K number of folds by:

$$D_{KL}(P\|Q) = \int_X P(x) \log \left(\frac{Q(x)}{P(x)} \right) dx \quad (12)$$

If we assume $P(x; \theta)$ as true distribution for given input X with parameter θ and $Q(x; \hat{\theta})$ as arbitrary target distribution with parameter $\hat{\theta}$ then we can rewrite D_{KL} as:

$$D_{KL}(P(\cdot; \theta) \| Q(\cdot; \hat{\theta})) = \mathbb{E}_{X \sim P(\cdot; \theta)} \left[\log \left(\frac{Q(X; \hat{\theta})}{P(X; \theta)} \right) \right] \quad (13)$$

Consider the special case of $Q(x; \hat{\theta})$ parameterized by $\hat{\theta}$ whereby we want to minimize D_{KL} w.r.t $\hat{\theta}$. For this case D_{KL} is at minimum if we have $Q(x; \hat{\theta}) = P(x; \hat{\theta})$. Thus we get:

$$D(P(\cdot; \theta) \| P(\cdot; \hat{\theta})) \geq 0 \quad (14)$$

By applying Taylor expansion up to second-order to the $\log P(x; \hat{\theta})$ for true parameter θ we have:

$$\begin{aligned} \log P(X; \hat{\theta}) &= \log P(X; \theta) \\ &+ (\hat{\theta} - \theta) \frac{\partial \log P(X; \theta)}{\partial \theta} \\ &- \frac{1}{2} (\hat{\theta} - \theta)^2 \frac{\partial^2 \log P(X; \theta)}{\partial \theta^2} + O((\hat{\theta} - \theta)^3) \end{aligned} \quad (15)$$

By taking expectation w.r.t X we have:

$$\begin{aligned} \mathbb{E}_{X \sim P(\cdot; \theta)} \left[\log P(X; \hat{\theta}) - \log P(X; \theta) \right] &= \\ (\hat{\theta} - \theta) \mathbb{E}_{X \sim P(\cdot; \theta)} \left[\frac{\partial \log P(X; \theta)}{\partial \theta} \right] & \\ - \frac{1}{2} (\hat{\theta} - \theta)^2 I(\theta) + O((\hat{\theta} - \theta)^3) & \end{aligned} \quad (16)$$

The left-hand in above mentioned equation is D_{KL} i.e $D(P(\cdot; \theta) \| P(\cdot; \hat{\theta}))$. As we know that D_{KL} is always non-negative, as so the right-hand side must also be non-negative. Thus we get:

$$\left(\frac{\hat{\theta} - \theta}{2} \right) I(\theta) \geq 0 \quad (17)$$

It will hold for any $\hat{\theta}$, from this we can conclude that:

$$I(\theta) \geq 0 \quad (18)$$

which is Fisher information. The following algorithm 1 provides an overview of our proposed method C^3 .

B EXPERIMENTS

In this section, we demonstrate the efficacy of C^3 against multiple baseline settings for causal covariate shift and on the benchmarks for natural covariate shift as a surrogate.

1. Baselines:

There are five baselines in our experiment:

- **B1:** *Clean* Verifying the effectiveness of C^3 on datasets without any covariate shift.

Algorithm 1 Dataset fragmentation and causal covariate shift correction

Require: model $f(\theta)$ parameterized by θ ;
training dataset \mathcal{D}_{tr} ;
validation data \mathcal{D}_v ;
number of batches K ;
number of epochs T ;

- 1: **procedure** SHIFTCORRECTION($\mathcal{D}_{tr}, \mathcal{D}_v$)
- 2: Split \mathcal{D}_{tr} into K batches
- 3: Initialize $f(\theta)$ and $\mathcal{L}(x, y; \theta)$
- 4: **for** epoch $\leftarrow 1$ **to** T **do**
- 5: **for** $i \leftarrow 1$ **to** K **do**
- 6: **for** $j \leftarrow i + 1$ **to** K **do**
- 7: Compute $D_{KL}(D_i, D_j)$
- 8: **for each pair** (D_i, D_j) :
- 9: $\mathcal{L}(x, y; \theta) =$
- 10: $-\int P(y(x)) \log(P(y|x; \theta)) d\theta$
- 11: $-\lambda \times \int \frac{\partial^2 \log p(X|\theta)}{\partial \theta \partial \theta^T} d\theta$
- 12: **end for**
- 13: **end for**
- 14: Update $f(\theta)$ using $\mathcal{L}(x, y; \theta)$
- 15: **end for**
- 16: **return** $f(\theta)$
- 17: **end procedure**

- **B2: Natural shift Consequences** Analyzing the performance of the C^3 in the presence of natural covariate shift.
 - **B3: Causal shift Consequences** Analyzing C^3 performance in the presence of causal shift caused by dataset fragmentation.
 - **B4: Loss Recalibration** Recalibrating the loss function and then measure the performance of C^3 .
 - **B5: Correction** correction of natural covariate shift via proxy with C^3 .
2. **Model architecture:** We used a five-layer convolutional neural network (CNN) with soft-max cross-entropy loss. Our CNN model consists of 2 convolutional layers with pooling, and 3 fully connected layers. The model architecture for all image-based benchmarks remains consistent, for tabular datasets the model architecture differs from image-based but remains the same for all tabular datasets. We used a multi-layer perceptron network for tabular data with a hidden layer with 4 neurons, relu as an activation function, and Adam optimizer. We set the hyper-parameter λ value within the range (0.01, 0.04, 0.07, 0.1) in all of our experiments. We present $\lambda = 0.1$ results in this paper for all of our experiments. All of our baselines are implemented in TensorFlow 2.11 ¹ and the code is anonymously available at ².
 3. **Machine Specification:** We run all of our experiments on RTX 3090 Ti with 24 GB GPU memory and 128 GB system memory.
 4. **Benchmarks:** We compare the performance of C^3 with standard cross validation and significant importance based methods like: importance weighting (IW) Huang et al. (2006), importance weighting cross-validation (IWCV) Sugiyama et al. (2007a), kernel mean matching (KMM) Gretton et al. (2009) and dynamic importance weighting (DIW) Fang et al. (2020). They were strategically chosen to represent landmark literature and current state-of-the-art.
 5. **Datasets:** To compare the effectiveness of our developed method C^3 we used 40 real-world benchmarking datasets. To evaluate our method we used 13 image-based datasets benchmarks and 27 binary datasets from KEEL repository as benchmarks Alcalá-Fdez

¹www.tensorflow.org²https://anonymous.4open.science/r/C3-C908/MNIST-Batchwise

et al. (2011). The used image-based benchmarks, comprising: MNIST LeCun (1998), Fashion-MNIST Xiao et al. (2017), Kuzushiji-MNIST Clanuwat et al. (2018), Permuted-MNIST Goodfellow et al. (2013), MNIST-C Mu & Gilmer (2019), SVHN Netzer et al. (2011), Caltech101 Fei-Fei et al. (2004), Tiny ImageNet Krizhevsky et al. (2009), STL-10 Coates et al. (2011) CIFAR-10 and CIFAR-100 Krizhevsky et al. (2009), CIFAR10-C and CIFAR100-C Hendrycks & Dietterich (2019).

6. **Calibrating the penalty:** One of our contributions to the paper is introducing the penalty term as above mentioned. We calibrate the penalty term (λ) with different values in batch/fold setup and present the result in Fig 1. We report $\lambda = 0.1$ results in our paper because our method C^3 is more robust to covariate shift. In figure 1 we can observe that C^3 performs better when we set $\lambda = 0.1$ as compared to other values.

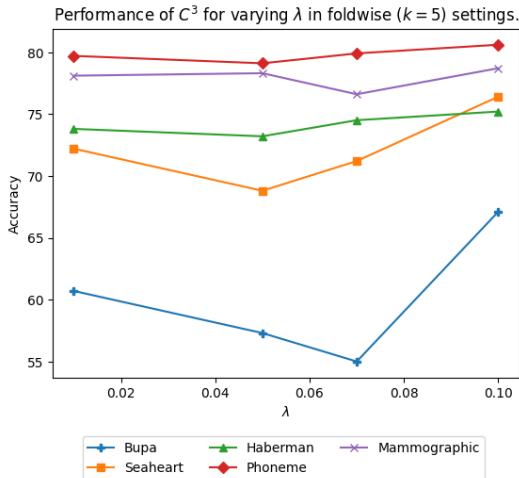


Figure 1: Performance of C^3 for varying λ in foldwise ($k = 5$) settings.

7. **Experimental design:** To study the effect of causal covariate shift caused by fragmentation, we perform evaluations on datasets with natural covariate shift and also on clean (free of covariate shift) datasets. We use accuracy as the first and direct evaluation metric in all experiments. We run each experiment 5 times and report average results due to spatial constraints.

C DISCUSSION

To verify the effectiveness of C^3 , we perform batchwise experiments for causal covariate shift whose results are presented in Table 2 which also validates **B4 & B5**. We consider batchwise holdout cross-validation as a baseline in comparison to C^3 . To ensure better performance of C^3 we compare the mean accuracy over all batches μ_1 of Table 3 and μ_2 of Table 2. We report accuracy for each single batch as well in all experimental settings to verify C^3 performance. We then consider C^3 with the whole dataset as a baseline for our C^3 batchwise method.

The Δ_3 of Table 2 presents the difference between μ_2 of Table 2 and μ_1 of Table 3. The Δ_3 shows improvement in accuracy and provides support to our claim of causal covariate shift correction **B5**. To verify **B5** we executed C^3 in batchwise settings on all dataset which results are reported in Table 2.

Our proposed method C^3 , shows improvement in accuracy in almost every batchwise setting and for each batch also as compared to the baseline. To validate the adaptive nature of C^3 to natural shift correction, we perform experiments on above mentioned datasets with natural shift. We notice that C^3 is able to correct natural shift when it tries to correct causal shift. C^3 shows improvement in accuracy for almost all benchmarks, like it shows 5%, 13.9%, and 8.6% improvement for Kuzushiji-MNIST, CIFAR10-C, and Fashion-MNIST with 20 batch split. C^3 also adapts to natural shift when

it tries to correct causal covariate shift.

C^3 's accuracy improves as the number of batches decreases, due to statistics getting more robust with larger supports. It is shown in Table 2. C^3 7.5% for Fashion-MNIST and 6.9% improvement in accuracy in 10 batch setup as compared to CV with the same batch setup. C^3 improves in accuracy with 7.2%, 7.2%, and 2.1% for Fashion-MNIST, Kuzushiji-MNIST, and Permuted-MNIST when batch size is 6. For the batch size 5, the improvement is 9.7%,8.1%, and 7.3% for CIFAR100, Kuzushiji-MNIST, and Fashion-MNIST. In 4 batches scenario we report 11.3%, 6.9%, 6.1%, and 5.8% improvement in accuracy for CIFAR-100, Khushiji-MNIST, Fashion-MNIST, and CIFAR100-C. In the case of 2 batches the improvement in accuracy is 20.3%, 15.5%, 6.6%, and 6.3% for CIFAR-10, CIFAR-10, CIFAR100-C, and Khushiji-MNIST. Overall, C^3 outperforms in the batchwise case and in the case where a complete dataset is provided with other benchmarking methods, and results are discussed ahead in the comparison with SOTA.

Dataset	Baseline		Batchwise accuracy						Mean μ_2	Variance σ_2^2	$\Delta_3 = \mu_2 - \mu_1$ $\Delta_3(\%)$
	CV	C^3	B1	B2	B3	B4	B5	B6			
Training data = 5% , Number of Batches = 20											
MNIST	94.8	97.9	90.7	90.6	91	91.7	91.4	91.8	91.2	0.09	↑ 2.5
Permuted-MNIST	95.1	97.6	91.1	89.8	90.2	90.4	91.5	90.7	90.3	0.26	↑ 1.9
Fashion-MNIST	83.1	88.4	81.5	81.7	81.2	81.4	81.5	81.9	81.5	0.058	↑ 8.6
Kuzushiji-MNIST	75.4	89.2	68.5	69.4	67.2	68	67.8	66.9	68.4	0.63	↑ 5.0
CIFAR-10	71.5	88.7	50.9	51.4	52.2	48.9	50.3	57.4	51.8	7.18	↑ 1.9
CIFAR-100	38.2	58.7	23.9	18.2	18.5	17.8	23.9	18.3	20.1	7.26	↑ 1.8
CIFAR10-C	63.9	73.3	46.4	54.3	57.8	61.1	61.5	61.8	57.2	30.1	↑ 13.9
CIFAR100-C	28.8	39.4	11.9	17.2	18.5	21.3	22.1	24.9	19.3	17.1	↑ 0.9
Training data = 10% , Number of Batches = 10											
MNIST	94.8	97.9	91.9	91.7	91.2	91.8	91.3	91.8	91.7	0.08	↑ 0.6
Permuted-MNIST	95.1	97.6	91.6	91.9	91.3	91.6	90.1	91.2	91.5	0.31	0
Fashion-MNIST	83.1	88.4	79.5	82.4	81.6	79.5	82.3	81.9	81.2	1.21	↑ 7.5
Kuzushiji-MNIST	75.4	89.2	71.4	70.4	71.7	70.7	70.5	70.9	70.9	0.71	↑ 6.9
CIFAR-10	71.5	88.7	52.1	53.1	48.5	59.3	52.5	55.7	53.5	11.09	↑ 0.9
CIFAR-100	38.2	58.7	27.2	25.8	20.4	17.0	21.9	22.8	22.5	11.3	↑ 1.0
CIFAR10-C	63.9	73.3	52.7	59.9	61.9	64.4	66.1	65.7	61.7	21.1	↑ 39.1
CIFAR100-C	28.8	39.4	16.2	22.1	24.8	27.2	26.8	27.3	21.1	15.6	↓ 1.7
Training data = 15% , Number of Batches = 6											
MNIST	94.8	97.9	93.2	92.6	93.2	93.5	93.1	93.3	93.2	0.09	↑ 1.7
Permuted-MNIST	95.1	97.6	93.1	93	92.7	93.7	93.5	93.1	93.2	0.13	↑ 2.1
Fashion-MNIST	83.1	88.4	81.4	81.9	82.9	80.9	82.3	82.2	81.9	0.49	↑ 7.2
Kuzushiji-MNIST	75.4	89.2	73.8	73.9	74.4	74.6	73.9	74.2	74.2	0.13	↑ 7.2
CIFAR-10	71.5	88.7	53.4	57.8	55.9	54.1	56.1	58.2	55.9	3.7	↑ 2.0
CIFAR-100	38.2	58.7	25.8	22.4	26.6	23.4	22.9	24.7	24.3	2.34	↑ 1.7
CIFAR10-C	63.9	73.3	58.4	61.1	63.2	64.3	67.4	66.9	63.5	9.87	↑ 42.4
CIFAR100-C	28.8	39.4	21.9	25.5	27.2	28.7	28.5	29.5	26.8	6.6	↑ 1.2
Training data = 20% , Number of Batches = 5											
MNIST	94.8	97.9	93.6	93.8	94.3	93.7	93.8	-	93.8	0.07	↑ 1.9
Permuted-MNIST	95.1	97.6	94.1	93.9	93.6	94.1	94.3	-	94	0.07	↑ 2.2
Fashion-MNIST	83.1	88.4	82.8	83.1	82.1	81.4	82.6	-	82.4	0.44	↑ 7.3
Kuzushiji-MNIST	75.4	89.2	75.4	76.3	75.8	75.1	75.6	-	75.6	0.21	↑ 8.1
CIFAR-10	71.5	88.7	50.3	56.2	53.5	57.8	59.9	-	55.5	11.3	↑ 18
CIFAR-100	38.2	58.7	34.2	35.4	33.9	34.9	34.7	-	34.6	11.7	↑ 9.7
CIFAR10-C	63.9	73.3	58.4	63.3	64.3	66.5	66.2	-	63.7	8.53	↑ 1.7
CIFAR100-C	28.8	39.4	22.1	25.4	27.4	28.9	29.7	-	26.7	7.43	↑ 2.9
Training data = 25% , Number of Batches = 4											
MNIST	94.8	97.9	94.4	94.4	94.3	94.4	-	-	94.4	0.003	↑ 2.0
Permuted-MNIST	95.1	97.6	94.4	94.3	94.5	94.5	-	-	94.4	0.009	↑ 2.8
Fashion-MNIST	83.1	88.4	82.8	83.2	83.6	83.5	-	-	83.3	0.13	↑ 6.1
Kuzushiji-MNIST	75.4	89.2	77.2	75.5	77.6	75.3	-	-	76.4	1.37	↑ 6.9
CIFAR-10	71.5	88.7	56.8	57.3	62.2	63.4	-	-	59.9	8.47	↑ 5.0
CIFAR-100	38.2	58.7	33.9	34.1	34.7	33.5	-	-	34.1	0.18	↑ 11.3
CIFAR10-C	63.9	73.3	60.9	64.4	66.8	68.3	-	-	65.1	7.81	↑ 3.7
CIFAR100-C	28.8	39.4	24.7	28.2	29.7	31.9	-	-	28.6	6.86	↑ 5.8
Training data = 50% , Number of Batches = 2											
MNIST	94.8	97.9	95.9	96.1	-	-	-	-	96	0.02	↑ 2.5
Permuted-MNIST	95.1	97.6	95.7	96.1	-	-	-	-	95.9	0.08	↑ 2.4
Fashion-MNIST	83.1	88.4	84.2	84.4	-	-	-	-	84.3	0.02	↑ 4.5
Kuzushiji-MNIST	75.4	89.2	79.3	80.4	-	-	-	-	79.8	0.61	↑ 6.3
CIFAR-10	71.5	88.7	76.3	80.6	-	-	-	-	78.4	4.62	↑ 20.3
CIFAR-100	38.2	58.7	39.8	39.9	-	-	-	-	39.85	.002	↑ 15.5
CIFAR10-C	63.9	73.3	65.5	68.6	-	-	-	-	67.1	2.4	↑ 2.8
CIFAR100-C	28.8	39.4	31.2	34.8	-	-	-	-	33	3.24	↑ 6.6

Table 2: C^3 Batchwise Accuracy

Dataset	Baseline		Batchwise accuracy						Mean	Variance
	CV	C^3	B1	B2	B3	B4	B5	B6	μ_1	σ_1^2
Training data = 5% , Number.of.Batches = 20										
MNIST	94.8	97.9	88.1	89.3	87.9	89.9	88.9	88.8	88.7	0.49
Permuted-MNIST	95.1	97.6	88	86.1	88.9	88.7	87.2	88.3	88.4	1.41
Fashion-MNIST	83.1	88.4	72.7	73.7	74.2	72.5	74	70.6	72.9	1.94
Kuzushiji-MNIST	75.4	89.2	63.6	63.4	62.2	66.7	58.3	63.4	63.4	5.59
CIFAR-10	71.5	88.7	44.1	49.0	50.3	50.7	51.2	54.5	49.9	9.67
CIFAR-100	38.2	58.7	13.1	16.5	18.1	19.3	20.4	22.7	18.3	9.17
CIFAR10- C	63.9	73.3	19.3	20.1	16.3	16.1	14.9	10.2	16.2	10.4
CIFAR100- C	28.8	39.4	11.1	16.3	19.1	19.7	21.6	22.3	18.4	14.2
Training data = 10% , Number.of.Batches = 10										
MNIST	94.8	97.9	90.7	91.7	91.1	90.2	89.3	91.5	91.1	1.06
Permuted-MNIST	95.1	97.6	91.9	92.8	91.8	91.2	91.4	91.3	91.5	0.62
Fashion-MNIST	83.1	88.4	69.4	69.9	75.2	73.4	74.4	71.7	73.7	9.22
Kuzushiji-MNIST	75.4	89.2	64	63.6	64.1	64.9	65.2	64.5	64.0	1.15
CIFAR-10	71.5	88.7	47.9	52.8	52.9	53.7	54.5	54.1	52.6	4.87
CIFAR-100	38.2	58.7	17.3	20.3	22.2	23.3	24.7	21.2	21.5	5.51
CIFAR10- C	63.9	73.3	22.8	17.6	18.4	12.2	17.4	12.9	22.6	16.8
CIFAR100- C	28.8	39.4	15.5	21.9	25.2	26.6	27.1	20.5	22.8	16.3
Training data = 15% , Number.of.Batches = 6										
MNIST	94.8	97.9	90.8	90.7	91.7	92.2	92.2	91.6	91.5	0.43
Permuted-MNIST	95.1	97.6	91.2	90.2	91.2	92.1	90.6	91.1	91.1	0.41
Fashion-MNIST	83.1	88.4	74.4	75.7	77.7	75	70.6	74.7	74.7	5.40
Kuzushiji-MNIST	75.4	89.2	66.9	67	66.4	69.9	64.8	67.2	67.0	2.73
CIFAR-10	71.5	88.7	50.9	51.2	53.9	53.8	57.1	56.9	53.9	5.91
CIFAR-100	38.2	58.7	18.2	21.1	22.5	23.4	24.1	24.4	22.6	4.57
CIFAR10- C	63.9	73.3	18.3	25.1	23.9	20.7	20.9	21.1	21.6	4.99
CIFAR100- C	28.8	39.4	18.2	19.9	21.2	21.9	25.6	27.1	22.3	9.64
Training data = 20% , Number.of.Batches = 5										
MNIST	94.8	97.9	92.7	92.2	93.4	91.2	90.2	—	91.9	1.59
Permuted-MNIST	95.1	97.6	91	91.7	91.4	91.2	93.5	—	91.8	1.01
Fashion-MNIST	83.1	88.4	76.7	74.1	72	75.3	77.2	—	75.1	4.40
Kuzushiji-MNIST	75.4	89.2	68.3	69.2	67.7	65.5	66.8	—	67.5	2.02
CIFAR-10	71.5	88.7	36.9	38.5	37.5	36.8	37.9	—	37.5	0.50
CIFAR-100	38.2	58.7	19.7	22.3	23.5	24.4	24.9	—	22.9	3.43
CIFAR10- C	63.9	73.3	58.1	62.0	61.8	60.7	67.5	—	62.0	9.43
CIFAR100- C	28.8	39.4	20.0	23.2	23.2	26.7	26.1	—	23.8	5.77
Training data = 25% , Number.of.Batches = 4										
MNIST	94.8	97.9	92.1	93.6	92.5	91.3	—	—	92.4	0.92
Permuted-MNIST	95.1	97.6	92.1	92.2	90.5	91.6	—	—	91.6	0.61
Fashion-MNIST	83.1	88.4	74.6	77.5	78.1	78.5	—	—	77.2	3.12
Kuzushiji-MNIST	75.4	89.2	70.6	69.2	69.5	68.8	—	—	69.5	0.60
CIFAR-10	71.5	88.7	51.9	52.7	56.9	58.1	—	—	54.9	7.02
CIFAR-100	38.2	58.7	20.3	22.4	23.9	24.8	—	—	22.8	2.7
CIFAR10- C	63.9	73.3	57.6	62.1	63.1	62.6	—	—	61.4	4.81
CIFAR100- C	28.8	39.4	19.7	23.4	23.8	24.5	—	—	22.8	3.64
Training data = 50% , Number.of.Batches = 2										
MNIST	94.8	97.9	93.3	93.7	—	—	—	—	93.5	0.08
Permuted-MNIST	95.1	97.6	93.3	93.7	—	—	—	—	93.5	0.08
Fashion-MNIST	83.1	88.4	80	79.7	—	—	—	—	79.8	0.04
Kuzushiji-MNIST	75.4	89.2	73.6	73.3	—	—	—	—	73.5	0.04
CIFAR-10	71.5	88.7	56.2	60.1	—	—	—	—	58.1	3.81
CIFAR-100	38.2	58.7	23.2	25.4	—	—	—	—	24.3	1.21
CIFAR10- C	63.9	73.3	63.2	65.5	—	—	—	—	64.3	1.32
CIFAR100- C	28.8	39.4	25.3	27.5	—	—	—	—	26.4	1.21

Table 3: CV batch-wise accuracy